Rotational Spectrum of NSF_3 in the Ground and $v_5 = 1$ Vibrational States: Observation of Q-Branch Perturbation-Allowed Transitions with $\Delta(k - l) = 0, \pm 3, \pm 6$ and Anomalies in the Rovibrational Structure of the $v_5 = 1$ State

Sven Macholl,[†] Heinrich Mäder,*[,†] Hauke Harder,[†] Laurent Margulès,[‡] Pascal Dréan,[‡] Jean Cosléou,[‡] Jean Demaison,[‡] and Petr Pracna[§]

Institut für Physikalische Chemie, Universität Kiel, Olshausenstrasse 40-60, 24098 Kiel, Germany, Laboratoire de Physique des Lasers, Atomes et Molécules, UMR CNRS 8523, Université de Lille I, 59655 Villeneuve d'Ascq, France, and J. Heyrovský Institute of Physical Chemistry, v.v.i., Academy of Sciences of the Czech Republic, 18223 Prague 8, Czech Republic

Received: August 16, 2008; Revised Manuscript Received: October 25, 2008

The rotational spectrum of NSF_3 in the ground and $v_5 = 1$ vibrational states has been investigated in the centimeter- and millimeter-wave ranges. R-branch ($J + 1 \leftarrow J$) transitions for $J = 0$, 1 and Q-branch rotational transitions for the $v_5 = 1$ vibrational state have been measured by waveguide Fourier transform microwave spectroscopy in the range 8−26.5 GHz. The *Q*-branch transitions include 28 direct *l*-type doubling transitions ($kl = +1$, A_1) ↔ ($kl = +1$, A_2) with $J \leq 62$, and 108 direct *l*-type resonance transitions following the selection rule $\Delta k = \Delta l = \pm 2$ with $J \leq 60$ and $G = |k - l| \leq 3$. A process called "regional resonance" was observed in which a cluster of levels interacted strongly over a large range in *J*. This process led to the observation of 55 perturbation-allowed transitions following the selection rules $\Delta(k - l) = \pm 3, \pm 6$. In particular, ($kl = +1$, A_+) ↔ ($kl = -2$, A_-), ($kl = +4$, A_+) ↔ ($kl = +1$, A_-), ($kl = +2$) ↔ ($kl = -1$), ($kl = +3$) ↔ ($kl = 0$), ($kl = +2$) ↔ ($kl = -3$), and ($kl = +3$) ↔ ($kl = -3$). The various aspects of the regional resonances are discussed in detail. An accidental near-degeneracy of the $kl = 0$ and $kl = -4$ levels at $J = 26/27$ led to the observation of perturbation-allowed transitions following the selection rule $\Delta(k-l) = \pm 6$ with ($kl = +2$) ↔ ($kl = -4$). A corresponding near-degeneracy between $kl = -1$ and $kl = -3$ levels at $J = 30/31$ led to the detection of similar transitions, but with ($kl = +3$) ↔ ($kl = -3$). In the range 230−480 GHz, R-branch rotational transitions have been measured by absorption spectroscopy up to $J = 49$ in the ground-state and up to $J = 50$ in the $v_5 = 1$ vibrational state. The transition frequencies have been analyzed using various reduced forms of the effective Hamiltonians. The data for the $v_5 = 1$ vibrational state have been fitted successfully using two models up to seventh order with $\Delta k = \pm 3$ interaction parameters constrained (d_t constrained to zero, and ε to zero or to the ground-state value). On the other hand, reductions with the ($\Delta k = \pm 1$, $\Delta l = \mp 2$) interaction parameter q_{12} fixed to zero failed to reproduce the experimental data since the parameters defining the reduction transformation do not arise in the correct order of magnitude. The ground-state data have been analyzed including parameters up to fourth order constraining either parameters of the $\Delta k = \pm 3$ interactions to zero (reduction A), or of the $\Delta k = \pm 6$ interactions to zero (reduction B). The unitary equivalence of the different parameter sets obtained is demonstrated for both vibrational states.

1. Introduction

In a series of investigations of C_{3v} symmetric top molecules in an isolated singly excited vibrational state of a degenerate vibration ($v_t = 1$), it has been shown that it is possible to fit data sets with parameter sets of different reductions which are unitary equivalent. This method has also been applied to the nondegenerate vibrational states. Two reductions have been proposed for the analysis of the nondegenerate states and three reductions for the singly exited degenerate vibrational states.[1,2]

For each reduction scheme considered, the parameters characterizing the Hamiltonian take on effective values which represent linear combinations of several molecular constants. In order that the particular reduction employed is suitable to fit the data set, the parameters defining the reduction transformation have to arise in the correct order of magnitude.[1] Otherwise, the reduction might fail to produce an acceptable model. The failure is typically characterized either by an inability to reproduce the data within the experimental accuracy, or by the need to include a large number of higher order parameters, resulting in problems with correlations between the parameters and slow convergence of the fit. The most common cases of such failures arise for symmetric top molecules close to the spherical top limit. For such molecules, owing to the small magnitude of $A - B$ (or $C - A$), those terms arising from the reduction transformation exceed the order-of-magnitude limit if the $\Delta k = \pm 3$ interaction parameter ε is constrained to zero. Therefore this constraint should be avoided. In an investigation of rotational spectra of OPF_3 in the ground vibrational state, Styger et al.[3] have presented a stringent test on this process. They have shown that a reasonable reproduction of the data was not possible if ε was

* Corresponding author. E-mail: maeder@phc.uni-kiel.de. Telephone: +49 431 581711. Fax: +49 431 8801704.
† Institut für Physikalische Chemie, Universität Kiel.
‡ Laboratoire de Physique des Lasers, Atomes et Molécules, UMR CNRS 8523, Université de Lille I.
§ J. Heyrovský Institute of Physical Chemistry, v.v.i., Academy of Sciences of the Czech Republic.

10.1021/jp807342f CCC: $40.75
Published on Web 01/05/2009

fixed at zero, and that the models with ε varied were of significantly better quality. For other quasi-spherical symmetric top molecules such as SbH_3,[4] it has been shown that models making use of the constraint $\varepsilon = 0$ needed a significantly larger set of parameters to obtain a reasonable quality of the fit. Problems in the use of reductions have also been reported for isolated singly excited degenerate vibrational states of C_{3v} symmetric top molecules. Pracna et al.[5] have reported the failure of reduction *D* (see ref 1) for CDF_3 in the vibrational state $v_5 = 1$; in this case, several parameters were highly correlated. These correlations could be explained as arising from the rather small value of the ($\Delta l = \Delta k = \pm 2$) interaction constant q_{22} which made the reduction transformation break the order-of-magnitude limits in reduction *D*.

The molecule thiazyl trifluoride, NSF_3, can be regarded as an intermediate case. With a value of $(A - B) \cong 550$ MHz and a value of $\gamma = 2(A - B)/(A + B) = 0.11$, it is rather close to the spherical top limit, but is not an extreme case like $FCl^{18}O_3$ ($\gamma = 0.03$), OPF_3 ($\gamma = 0.05$), or SbH_3 ($\gamma = 0.05$). For NSF_3, γ is closer to PH_3 ($\gamma = 0.13$) or $FCl^{16}O_3$ ($\gamma = 0.12$). Previous investigations of rotational spectra in the vibrational state $v_6 = 1$ gave indications that standard models may fail to reproduce observed spectra for NSF_3.[6] In the $v_6 = 1$ state, Small and Smith had to refine both q_{12} and ε in fitting spectra which included ($\Delta k = \pm 3$) Q-branch perturbation-allowed transitions in the radio frequency range.[7] It was found that some of the constants determined were highly correlated. Thus NSF_3 seemed to be a good candidate for testing the various models of reductions both in the ground and degenerate vibrational states. Furthermore, the molecular constants and the thermal population for $v_5 = 1$ and $v_6 = 1$ seemed to allow the observation of high-resolution Q-branch rotational spectra for the ground-state as well as the $v_5 = 1$ and $v_6 = 1$ excited states. It might then well be possible to use Fourier transform microwave (FTMW) spectroscopy to measure ($\Delta k = \pm 3$) transitions in the ground-state and direct *l*-type resonance transitions in the excited states with the high accuracy necessary to carry out a stringent test on the models of reduction. However, we have only succeeded in obtaining and assigning Q-branch spectra for the $v_5 = 1$ vibrational state. For both the ground and $v_5 = 1$ vibrational states, R-branch spectra have been recorded as well. The data for each of the two vibrational states have been analyzed separately.

As will be shown, the rovibrational structure of the $v_5 = 1$ vibrational state shows clustering of energy levels at low values of $K = |k|$ leading to resonances extending over a large range in *J*. These "regional resonances" led to the observation of perturbation-allowed Q-branch rotational transitions following the selection rules $\Delta(k - l) = \pm 3, \pm 6$; these transitions occurred in several series which were followed over many values of *J*. To our knowledge, this phenomenon has not been previously observed for any other symmetric top molecule in an isolated excited vibrational state. Furthermore, these resonances allowed the observation of anomalous splittings in the hyperfine structure of transitions with E-symmetry owing to the lifting of the parity-degeneracy by the "tensor" terms in the spin-rotation interaction off-diagonal in *k*, as reported, for example, for PH_3 in ref 8. The regional resonance will be discussed in terms of eigenvectors of the affected levels in section 5, while the analysis of the hyperfine components will be given in a forthcoming paper.[9]

The hyperfine-free frequencies determined for the transitions could not be fitted with reductions in which the parameter q_{12} of the ($\Delta l = \pm 2, \Delta k = \mp 1$) interaction was constrained to zero. A possible reason for this failure will be discussed in section 5.

Both ground and excited-state data have been analyzed using two different reductions. In section 4, the unitary equivalence of the parameter sets obtained is shown, thus demonstrating the correctness of the models applied.

2. Experimental Section

The sample was provided by Professor R. Mews of the University of Bremen and was purified from more volatile compounds by typically three freeze−pump−thaw cycles.

Absorption spectrometers employing phase stabilized Thomson-CSF backward-wave oscillators were used between 340 and 480 GHz to record the millimeter wave rotational spectra. At lower frequencies measurements were done with harmonics of gunn diodes. The detection was carried out using helium-cooled InSb bolometers except for measurements around 230 GHz where superheterodyne detection was used. Measurements were performed at ambient temperatures and at pressures between 1 and 3 Pa.

Measurements in the centimeter wave range were performed using FTMW spectrometers in the ranges 8−18 and 18−26.5 GHz with rectangular and circular waveguides as sample cells.[1,10,11] The spectrometer running in the 8−18 GHz range used an oversized X-Band sample cell nominally working in the range 8−12 GHz. From 12 to 18 GHz, the sensitivity can be considerably lower due to increased reflections, so that only relatively strong transitions could be measured here with acceptable high quality. Typically pulses of 10 W and 0.5−1.2 μs were used to reach optimal conditions for the polarization of the molecular sample. Measurements were performed at ambient temperatures or 212 K and at pressures of typically 0.15 Pa. The transition frequencies and their experimental errors (three times the standard deviation) were determined from a least-squares fit of the time-domain data. For cases where the hyperfine structure had to be resolved (particularly where small splittings occurred), the required accumulation times were relatively long due to a reduced sample pressure (ca. 0.1 Pa) and the need for an improved signal-to-noise ratio. As a result, the number of such cases studied was limited. The center frequencies of these hyperfine multiplets were determined from the individual components in a process which was checked in most cases by the hyperfine analysis. Some transitions were measured at higher pressures, in which case only unresolved lines were obtained.

3. Spectra

R-Branch Rotational Spectra in the Ground and $v_5 = 1$ State. On the basis of constants reported by Small and Smith,[6] rotational spectra for $J + 1 \leftarrow J$ were predicted and measured by absorption spectroscopy for the ground and $v_5 = 1$ vibrational states up to $J = 49$, $K = |k| = 49$ and $J = 50$, $K = 50$, respectively. The corresponding spectra for $J = 0$ and 1 fall in the range of the FTMW spectrometer but, mainly for technical reasons, for the ground-state only the $J = 0$ and for $v_5 = 1$ the $J = 1$ transition was measured with this instrument. The recorded spectra follow qualitatively the description by Small and Smith,[6] except that the measurements were extended to higher values of *J* and *K*. For the ground state, ($K = 3$) splittings were observed for $J = 47-49$. These splittings arise from off-diagonal interactions and the associated parameters therefore become determinable. For the $v_5 = 1$ vibrational state, the resonances are much stronger at higher *J*, and consequently the

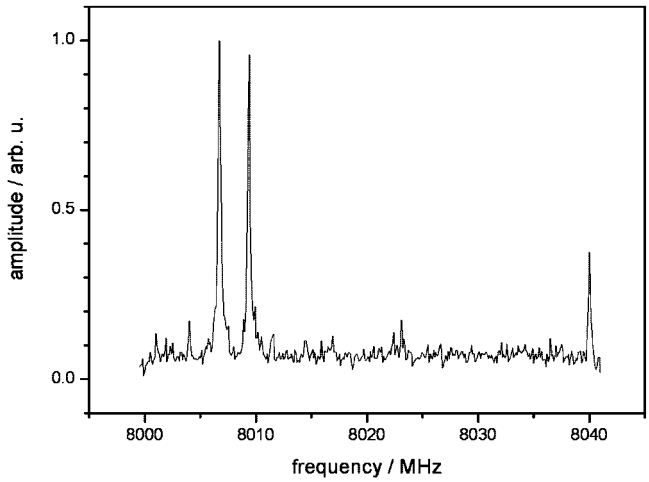

Figure 1. Amplitude spectrum in the range 8000−8040 MHz using microwave Fourier transform spectroscopy. The two strong lines at about 8006.7 and 8009.4 GHz are the direct *l*-type resonance transitions in the vibrational state $v_5 = 1$ of NSF_3 with $J = 34$, $G = 0$ and $J = 24$, $G = 1$, respectively.

assignment for a few lines was not straightforward. Furthermore, the observation of rovibrational splittings in the spectra at higher J for $kl = -2$ and $kl = +4$ yielded additional information on the $\Delta k = \pm 6$ interaction, information which is otherwise difficult to be obtained solely from R-branch rotational transitions.

The experimental frequencies of the transitions are given in the Supporting Information (see Tables S1 and S2).

Q-Branch Rotational Spectra in the Vibrational State $v_5 = 1$. ***Direct l-Type Resonance Transitions.*** Direct *l*-type resonance transitions are observable due to the mixing of states by the (2,2) *l*-type interaction, which couples states with the same value of $G = |k - l|$. This can lead to rather global resonances with very pronounced effects at low K and high J. Direct *l*-type resonance transitions can in general be observed if the (2,2) interaction parameter q_{22} is relatively large in magnitude and $|A - B - A\zeta|$ is small. Both the vibrational states with $v_5 = 1$ and $v_6 = 1$ meet these requirements. For $v_5 = 1$, although $|A - B - A\zeta|$ ($\approx$1700 MHz) is larger than for any molecule for which direct *l*-type resonance transitions have been previously measured, $|q_{22}| \approx 1.7$ MHz is large enough to compensate. For $v_6 = 1$, $|q_{22}|$ is not large ($\approx$0.25 MHz), but $|A - B - A\zeta|$ is relatively small ($\approx$813 MHz). Furthermore, both states are well populated at room temperature.[6]

We started the investigation with broadband scans around 8 GHz using a FTMW spectrometer operating in the scan mode.[10] In this region, we predicted lines for the ground-state as well as the $v_5 = 1$ and $v_6 = 1$ vibrational states. With a value of $(A - B) \approx 550$ MHz, ground-state forbidden transitions are predicted with $(k = \pm 4) \leftrightarrow (k = \pm 1)$ around 8000 MHz, as well as several transitions for the $v_6 = 1$ state and a few lines of the $G = 0$ and $G = 1$ bands of $v_5 = 1$. A few strong lines with comparable intensities were observed corresponding to the number of lines predicted for $v_5 = 1$. A typical spectrum is shown in Figure 1. In these spectra, the $G = 0$ lines could be easily assigned, while the lines expected to belong to the $G = 1$ band showed deviations from the predictions with no simple dependence on J. These deviations could be explained by a strong resonance between the $kl = -1$ and $kl = -3$ states. After some trial refinements, the lines could finally be assigned to the $G = 1$ band. With improved parameters, transitions were predicted more precisely and measurements were extended up to $J = 62$ and $G = 3$.

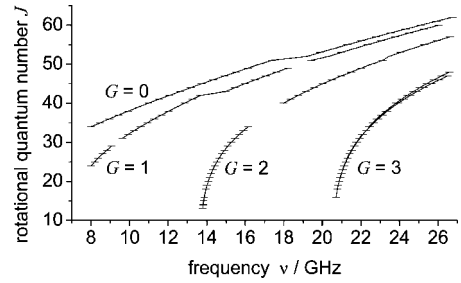

Figure 2. Fortrat diagram of the direct *l*-type resonance transitions observed for NSF_3 in the vibrational state $v_5 = 1$.

Nevertheless, the assignment was not straightforward. One of the problems was that some of the transitions had irregular hyperfine structure that was not initially understood and the hyperfine-free (center) frequencies could not be determined accurately. These transitions could be taken into account only after significant improvement in the understanding and analysis of the patterns observed. Another problem is reflected in the Fortrat diagram given in Figure 2. There are clear discontinuities in the $G = 0$ series at $J = 50$ and in the $G = 1$ series at $J = 43$, as well as less obvious discontinuities in the series with both $G = 1$ and 2 at $J = 52$. At each discontinuity, there is an overall shift of the transition frequencies from a specific value of J on. These shifts can be to higher frequency as for $G = 0$ or to lower as for $G = 2$. The value of J at the discontinuity appeared to be somewhat arbitrary since the labeling of the levels around this J-value was quite sensitive to the model. None of the frequency shifts characteristic of typical level crossings could be found. To our knowledge, such behavior has not been previously reported for similar spectra in symmetric top molecules. The origin of this anomaly lies in the resonance referred to throughout this paper as 'regional' and is discussed below.

Finally, the $G = 3$ transitions were found to be split due to various rovibrational interactions. The observed splittings reached a maximum value of 320 MHz for $J = 47$. For $J = 48$, the calculated splitting is larger, but only one component was measured.

Regional Resonance Transitions with $\Delta(k - l) = \pm 3, \pm 6$. If the discontinuity in the Fortrat diagram for $G = 0$ is neglected, the branch for J-values below the discontinuity can be extended continuously to higher values of J. For J-values on this branch above the discontinuity, the lines observed follow the selection rule $\Delta(k - l) = \pm 3$. The transitions result from strong resonances extending over large ranges of J (regional resonances) as discussed below. Similar perturbation-allowed transitions could be measured above each discontinuity. The specific selection rules followed for the transitions observed are as follows: $(kl = +1, A_+) \leftrightarrow (kl = -2, A_-)$ for $J = 50-62$; $(kl = +4, A_+) \leftrightarrow (kl = +1, A_-)$ for $J = 34-39, 43-49$; $(kl = +2) \leftrightarrow (kl = -1)$ for $J = 46-52$; $(kl = +3) \leftrightarrow (kl = 0)$ for $J = 43-54$; $(kl = +2) \leftrightarrow (kl = -3)$ for $J = 38, 41, 43-47, 51$; and $(kl = +3) \leftrightarrow (kl = -3)$ for $J = 41, 42$. The various branches are shown in Figure 3 for A_1,A_2 (a) and E symmetry (b).

Local Resonance Transitions with $\Delta(k - l) = \pm 6$. In addition, four transitions due to local resonances were observed. An accidental near-degeneracy of the $(kl = 0)$ and $(kl = -4)$ levels at $J = 26, 27$ allowed the measurement of transitions with the detailed selection rule $(kl = +2) \leftrightarrow (kl = -4)$, which corresponds to $\Delta(k\text{-}l) = \pm 6$. Similar transitions following the detailed selection rule $(kl = +3) \leftrightarrow (kl = -3)$ were observed for $J = 30, 31$ as a result of a local resonance between the $(kl = -1)$ and $(kl = -3)$ levels.

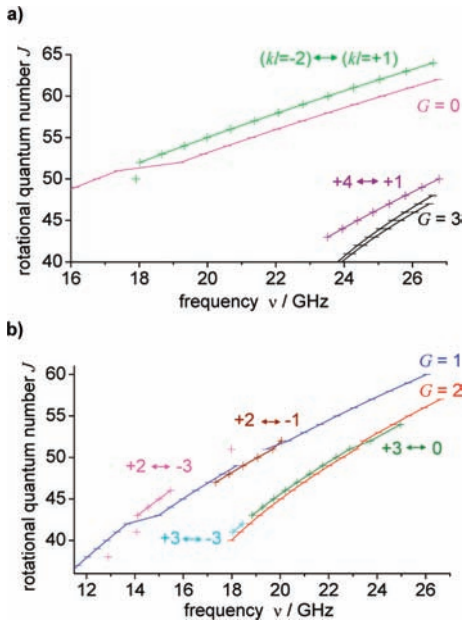

Figure 3. Fortrat diagram of Q-branch transitions observed for NSF_3 in the vibrational state $\upsilon_5 = 1$. (a) $A_{1/2}$ symmetry; (b) E symmetry.

Some of the Q-branch transitions appeared as multiplets due to the ^{14}N and ^{19}F hyperfine interactions. A detailed description and analysis will be given in a forthcoming paper.[9] The center frequencies calculated from these multiplets are given in the Supporting Information (see Table S2). For some multiplets it occurred that hyperfine components were missing or overlapping. In these cases the observed hyperfine lines could not be assigned unambiguously which lead to larger errors on the center frequencies and correspondingly to lower weights for these data in the fit (see below).

Closed Loops in the range of regional resonances. The shift of the branches at the discontinuities in Figures 2 and 3 corresponds to the frequency difference between the direct *l*-type resonance transitions and their counterparts following the selection rules $\Delta(k - l) = \pm 3$ or ± 6. This shift is the energy level difference between interacting levels in the range of the regional resonances, a difference which could therefore be precisely determined. For E-symmetry, these differences have been determined by two sets of transitions forming a closed loop allowing the application of the Ritz principle. Besides the direct *l*-type resonance transitions with $G = 1, 2$, there are four further types of transitions observable. In Figure 4, we have indicated the various transitions observed due to the regional resonance. It is worth noting that no transitions could be detected between the $kl = +3$ level and the upper level of the three lower levels indicated (level c), so that closed loops of transitions could only be obtained involving the lower energy level difference of $kl = 0$ and $kl = -1$. The transitions forming the closed loops are the direct *l*-type resonance transitions with $G = 1$ and 2 and the $\Delta(k - l) = \pm 3$ transitions with $(kl = +3) \leftrightarrow (kl = 0)$ and $(kl = +2) \leftrightarrow (kl = -1)$ for $J = 46-49$, 51 and 52. The Ritz principle has been tested on these closed loops by calculating the energy differences of the $kl = 0$ and $kl = -1$ levels using two different sets of transitions. Alternatively, one could have also calculated the difference of the $kl = +2$ and $kl = +3$ levels. As shown in Table 1, one finds excellent agreement for the differences experimentally obtained even though their determination was difficult due to irregularities in the hyperfine structure. In fact, the application of the Ritz principle to the hyperfine components has been a very helpful tool in understanding the various different types of hyperfine spectral patterns.

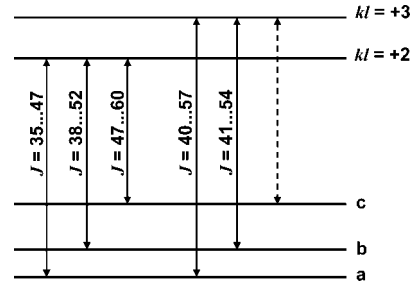

Figure 4. Energy level scheme showing perturbation-allowed transitions in the range of the regional resonance for symmetry E. Level a corresponds in reduction *D* to $kl = -1$ for $35 \le J \le 51$ and $kl = 0$ for $J \ge 52$, level b to $kl = -3$ for $35 \le J \le 42$, $kl = 0$ for $43 \le J \le 51$ and $kl = -1$ for $J \ge 52$, and level c to $kl = 0$ for $35 \le J \le 42$, $kl = -3$ for $J \ge 43$.

4. Multiple Fitting Analysis

The Ground Vibrational State. The data set for the ground-state included 96 transitions measured by Small and Smith[6] and 134 transitions recorded in this work. The transition frequencies were fitted with the program SIMFIT[5] using the matrix elements as given in the Appendix in a symmetrized basis set according to the symmetry species A_1, A_2, and E. The data were included with a weight proportional to the inverse square of the experimental error assumed. Two fits were performed with parameter sets corresponding to the reductions described by Aliev and Aleksanyan[12] (reduction A) and by Sarka[13] (reduction B). In reduction A, the data are fitted with the parameters characterizing the $\Delta k = \pm 3$ matrix elements (ε,ε_J) fixed to zero. In reduction B, the parameter characterizing the $\Delta k = \pm 6$ matrix elements (h_3) was fixed to zero. Parameters up to fourth order (sextic terms) have been refined. The rotational constant *A* was fixed to the value of 5194 MHz, which was obtained in the analysis of the $\upsilon_5 = 1$ state (see next section), while D_K and H_K were fixed to zero. In addition, in reduction B, the constants H_{JK} and ε_J were constrained to zero. In total, 7 parameters were fitted in reduction A, while 6 parameters were fitted in reduction B. In both reductions A and B, the quality of the fit was insensitive to signs for h_3 and ε, respectively. However, the analysis of the $\upsilon_5 = 1$ state clearly shows that the negative sign has to be taken for h_3. For ε, the positive sign has been assumed in accordance with the force field value of the related molecule OPF_3.[14] All transition frequencies were reproduced to within their experimental errors. In both reductions, the standard deviation was 20.5 kHz for data measured in this work, and 29.7 kHz for data of Small and Smith.[6] The values of the parameters obtained for each reduction are given in Table 2. The corresponding reproduction of the transition frequencies is given in Table S1 of the Supporting Information.

The unitary equivalence of two parameter sets is verified if the relations demonstrating the unitary equivalence are fulfilled and if the two fits are of comparable quality. Since the standard deviations for reductions A and B are essentially the same, one is left to check the fulfilment of the relations following from the theory of reduction, namely:

$$\xi = \frac{\Delta H_J}{2} = -\frac{\Delta H_{JK}}{18} = \frac{\Delta H_{KJ}}{30} = -\frac{\Delta H_K}{14} = \Delta h_3 = \frac{\Delta \varepsilon^2}{A - B} \tag{1}$$

where ΔP refers to the difference $P^B - P^A$ between the values obtained for parameter *P* using reductions *A* and *B*.

TABLE 1: Energy Level Differences ΔE of the $kl = 0$ and $kl = -1$ Levels Experimentally Obtained from Transitions Involving Upper Levels $kl = +2, +3$

	ΔE (MHz)					
upper level	$J = 46$	$J = 47$	$J = 48$	$J = 49$	$J = 51$	$J = 52$
$kl = +2$	283.598(70)	274.940(80)	267.707(73)	263.048(80)	264.419(3)	270.925(7)
$kl = +3$	283.637(20)	274.944(12)	267.723(12)	263.091(16)	264.424(12)	270.923(7)
Ritz principle	−0.039(90)	−0.004(92)	−0.016(85)	−0.043(96)	−0.005(16)	0.002(14)

TABLE 2: Parameters of the Effective Hamiltonian in the Vibrational Ground State of NSF_3 in Reductions A and B, where Standard Deviations Are Given in Units of the Least Significant Digit

parameter	unit	reduction A	reduction B
B	MHz	4636.24921 (15)	4636.24921 (15)
A	MHz	5194.0[a]	5194.0[a]
D_J	kHz	1.07692 (11)	1.07693 (10)
D_{JK}	kHz	2.12858 (19)	2.12850 (16)
D_K	kHz	0.0[a]	0.0[a]
H_J	mHz	0.2000 (222)	0.5179 (202)
H_{JK}	mHz	2.8467 (456)	0.0[a]
H_{KJ}	mHz	−1.7233 (465)	3.0039 (617)
H_K	mHz	0.0[a]	0.0[a]
ε	kHz	0.0[a]	0.2945 (197)
h_3	mHz	−0.1563 (389)	0.0[a]
no. of data		134	134
σ	kHz	20.5	20.4

[a] Constrained value.

TABLE 3: Demonstration of Unitary Equivalence of Parameter Sets Obtained for Reductions A and B in the Vibrational Ground State of NSF_3

term[a]	unit	verification
$^1/_2\Delta H_J$	mHz	0.1589 (212)
$-^1/_{18}\Delta H_{JK}$	mHz	0.1582 (25)
$^1/_{30}\Delta H_{KJ}$	mHz	0.1576 (36)
Δh_3	mHz	0.1563 (39)
$\Delta\varepsilon^2/(A - B)$	mHz	0.1555 (21)

[a] $\Delta P = P^B - P^A$.

In refs 2 and 3, the last expression in eq 1 was replaced by:

$$\xi = -2\frac{\varepsilon'\Delta\varepsilon}{(A-B)} \tag{2}$$

This is an approximation suitable only in the case of quasi-symmetric top molecules. It involves the true value of ε, here indicated with prime, which is not determinable from the fits and which has to be taken from force field calculations, if available. The last expression in eq 1, however, is obtained without approximation. It is not restricted to quasi-spherical tops and thus is of general use. If this expression is applied to the parameters from refs 3 and 4 to calculate ζ, its value is in much better agreement with the mean values obtained for the other expressions in eq 1. For OPF_3, we get $\xi = 1.67 \times 10^{-3}$ Hz using the last expression in eq 1, whereas the value of 1.78×10^{-3} Hz resulting from eq 2 is significantly different from the mean value of 1.68×10^{-3} Hz. This improvement was also noted in Table 4 of ref 3 with a very brief explanation in the footnotes. For SbH_3, the situation is similar to that in OPF_3. The value calculated with eq 1 is 6.16×10^{-10} cm^{-1}, compared to the mean value of 6.14×10^{-10} cm^{-1}, whereas the value obtained with eq 2 is 5.54×10^{-10} cm^{-1}. Work similar to that reported here was presented in ref 15 with respect to CH_3CF_3, a near-spherical rotor with $\gamma = 0.06$. This work on CH_3CF_3 also points out that, when the distortion dipole moment μ_D can be determined, the value of μ_D can (in favorable cases) be used to obtain the true magnitude of ε. Alternative expressions to the approximations given for ε_J and ε_K in eq 5 of ref 4 can be derived:

$$\xi = \Delta\varepsilon_J\frac{\varepsilon_A + \varepsilon_B}{D_J} = \frac{1}{2}\Delta\varepsilon_K\frac{\varepsilon_A + \varepsilon_B}{D_K} \tag{3}$$

In Table 3, experimental values obtained here for NSF_3 using eq 1 are compared. Excellent agreement is found, with all values agreeing within one standard deviation. This is true even for H_{JK}, which was constrained to zero in reduction B. Obviously, H_{JK} takes an accidentally small value in this reduction and constraining it to zero does not have a significant effect on the calculated difference. The verification of eq 1 for h_3 also confirms that the negative sign assumed for this parameter is correct. The results obtained here show that both reductions work equally well for NSF_3, a conclusion which was not necessarily expected beforehand due to the rather small value of $A - B$. Although the current data set might not be accurate enough to make a final judgment, it seems that the value of $A - B$ does not cause the transformation parameter t to exceed its order-of-magnitude limit. The slightly larger value of the parameter γ probably makes the constraints applicable to NSF_3 ($\gamma = 0.11$), constraints that are not useful for the related molecule OPF_3 ($\gamma = 0.05$).

TABLE 4: Parameters of the Effective Hamiltonian of the $v_5 = 1$ Level of NSF_3 in Reduction D and Model II, where Standard Deviations Are Given in Units of the Least Significant Digit

parameter	unit	reduction D	model II
B	MHz	4640.954071 (116)	4640.956917 (116)
A	MHz	5194.421323 (403)	5194.415613 (412)
D_J	kHz	1.0924409 (276)	1.0923954 (277)
D_{JK}	kHz	2.251405 (130)	2.251082 (132)
D_K	kHz	−1.6674 (185)	−1.6471 (189)
H_J	mHz	0.2[a]	0.5227[b]
H_{JK}	mHz	2.85[a]	−0.05752[b]
H_{KJ}	mHz	−1.723[a]	3.118[b]
H_K	mHz	0.0[a]	−2.259[b]
L_{JJK}	μHz	0.31562 (952)	0.27987 (973)
L_{JK}	μHz	−0.3902 (107)	−0.2714 (107)
$A\zeta$	MHz	−1 158.843014 (437)	−1 158.841427 (441)
η_J	kHz	41.911805 (515)	47.675224 (618)
η_K	kHz	−98.3996 (754)	−104.0959 (773)
τ_{JK}	Hz	1.62006 (615)	1.93541 (611)
τ_K	Hz	−10.350 (209)	−7.581 (215)
σ_J	μHz	0.0[b]	−4.188 (102)
σ_{JK}	μHz	−66.60 (136)	−89.03 (145)
σ_{KJ}	μHz	36.43 (338)	165.19 (260)
q_{22}	MHz	−1.697076444 (588)	−1.697071566 (645)
f_{22}^J	Hz	1.511616 (472)	3.683292 (482)
f_{22}^K	kHz	0.1339075 (406)	0.127163 (101)
f_{22}^{JJ}	μHz	13.3723 (869)	−26.6322 (900)
q_{12}	MHz	2.1121777 (112)	1.7861075 (116)
q_{12}^J	Hz	−37.41595 (419)	−52.56248 (438)
f_{42}	Hz	−1.707509 (125)	0.459057 (121)
f_{42}^J	μHz	12.7254 (573)	−25.7866 (574)
ε	kHz	0.0[b]	0.3[b]
h_3	mHz	−0.190830 (144)	−0.027293 (145)
no. of data (MMW/FTMW)		505/225	505/225
σ	kHz	33.8/1.18	33.0/1.20

[a] Constrained to the ground-state values. [b] Constrained values.

The Vibrational State $v_5 = 1$. Very accurate measurements have been performed for the $v_5 = 1$ vibrational state especially in the range 18−26.5 GHz. However, for many of the transitions with $\Delta J = 0$, the hyperfine multiplet was not sufficiently resolved to determine precise center frequencies. As a result, systematic errors occurred in the analysis and it was not possible to reproduce the Q-branch data within the "intrinsic" experimental errors obtained from the fits of the time-domain signals. Some of these hyperfine multiplets were remeasured under improved experimental conditions to resolve the hyperfine structure and obtain better agreement. In the final fits, some transitions for which the hyperfine structure was not or not fully resolved were included with reduced weight (errors of 20, 30, or 50 kHz) while other transitions, those at low J and the series with $G = 3$ (except below $J = 20$), were included with the obtained experimental errors.

The final data set consists of several types of data. The measurements taken with FTMW spectroscopy contribute 225 frequencies with an experimental error determined mostly from the fit of the time-domain signal (typically 1−5 kHz). Of these, 222 are Q-branch transitions. There are 163 transitions of the direct l-type resonance spectrum including both transitions following the selection rule ($\Delta k = \Delta l = \pm 2$) and direct l-doubling lines; 53 perturbation-allowed transitions with $\Delta(k - l) = \pm 3$; and 6 perturbation-allowed transitions with $\Delta(k - l) = \pm 6$. In addition, there are 3 frequencies for the $J = 2 \leftarrow 1$ transition. The measurements taken with absorption spectroscopy contribute 494 R-branch frequencies. Of these, 168 were reported by Small and Smith[4] with an accuracy of 50−400 kHz, and 326 were measured in the present study with a typical error of 50 kHz.

The vibrational states closest to the fundamental level with $v_5 = 1$ at 429 cm^{-1} are those with $v_6 = 1$ at 342 cm^{-1} and $v_3 = 1$ at 521 cm^{-1}. (The wave numbers are taken from ref 6.) Thus $v_5 = 1$ can be treated as an isolated state and an effective rovibrational Hamiltonian is suitable for the analysis. We have fitted the data using the program SIMFIT,[5] which builds up three Hamiltonian matrices according to A_1, A_2, and E symmetry using matrix elements of the rovibrational interactions up to seventh order as given in the Appendix. The matrices are subsequently diagonalized to obtain the eigenvalues and eigenvectors.

Three reductions have been proposed for fitting the experimental data of C_{3v} symmetric top molecules in a degenerate vibrational state with $v_t = 1$; see refs 1, 2, 16, and 17. In reduction D, the parameters of the k- and l-dependent (0,3) interactions (ε, d_t,...) are fixed at zero. In reduction Q, parameters of the (2, −1) and k-dependent (0,3) interaction (q_{12}, ε,...) are constrained to zero. In reduction QD, the parameters of the (2, −1) and l-dependent (0,3) interaction (q_{12}, d_t,...) are fixed at zero. Furthermore, it is recommended to constrain to zero all parameters corresponding to k-dependences of off-diagonal terms. All three reductions have been applied to the experimental data. However, the fits appeared to be rather difficult due to the strong resonances affecting a large number of transitions, and the convergence of the fits was rather slow. Another problem in fitting the data was that small changes in the parameters led to changes in the labeling of some of the states involved in transitions for several low values of K and in the millimeter wave data for some lines with high J and high K. This occurred in all reductions, but particularly in reductions Q and QD. In trial fits, parameters up to septic order were included. Nevertheless, reasonable fits were obtained only using reduction D. The fits using reductions Q and QD were of much poorer quality even when reduced data sets were used.

Several different attempts in fitting the data were made to obtain the most reasonable fits for reduction D. It was necessary to include parameters for diagonal terms up to seventh order (σ-Coriolis type constants), while for the off-diagonal terms parameters up to sixth order were sufficient. It has been shown in previous investigations that fitting f_{22}^K instead of one of the τ-constants leads to equivalent results and in some cases can be even the better choice, particularly if $|A - B - A\zeta|$ is small (for a detailed discussion, see Margulès et al.[18]). For the current data set, the best result was obtained with f_{22}^K fitted and τ_J constrained to zero.

With the H centrifugal distortion constants being varied, the best fit to the data was obtained, but the resulting values differed by up to 100% from their ground-state counterparts. To get a better agreement between ground and upper state parameters, we have finally constrained the H centrifugal distortion constants for $v_5 = 1$ to the ground-state values and fitted L_{JJK} and L_{JKK}, which then take on rather large values. (The values are around 10^{-13} MHz, rather than the 10^{-15} MHz expected.) When the constant σ_{KJ} was included, the convergence of the fit was slower and the stability was lower due to its correlation with τ_K. However, σ_{KJ} led to a slight but significant improvement of the fit and therefore was included in the analysis.

The best-fit parameters are given in Table 4. Most of the millimeter wave data were reproduced within the error limits assigned, with an exception of only a few lines of high K. The standard deviation of the millimeter wave data is 33.8 kHz. Systematic deviations for the Q-branch rotational transitions remained only for those lines where the hyperfine structure could not be sufficiently resolved. As mentioned above, the weight in such cases was reduced accordingly (e.g., for the series ($kl = +4$) ↔ ($kl = +1$)). Several lines of the series with $G = 3$ clearly could not be fit within the assigned experimental error. However, because the nonsystematic deviations remained well below 2 kHz and the data were of high quality, the weight has not been reduced in this case. The standard deviation of the fit of the FTMW data is 1.2 kHz.

In the course of investigation of the hyperfine structure, it appeared to be useful to apply a reduction different from those discussed above. We have carried out fits using a modified form of reduction D with ε constrained to the value determined for the ground state. This choice was based on the assumption that the sensitivity of ε to the transformation parameter t should be rather weak due to the small value of $A - B$ (see following section). As a result, the value of ε obtained in the ground-state fit is expected to be close to the true parameter, i.e., to the parameter in the unreduced effective Hamiltonian. This assumption is supported by the results obtained for OPF_3 and SbH_3.[3,4] A similar model has been applied by Graner et al.[19] in the fit of v_6 spectra of $FClO_3$ where the value of ε for $v_6 = 1$ was fixed to that of its ground-state counterpart. In the current work, this reduction will be called model II. In this model, the same parameters were varied as in reduction D, but with σ_J added and with the H constants constrained to values determined from eq 1. In model II, in contrast to the fits with reduction D, the inclusion of either f_{22}^K or τ_J led to equivalent results. Furthermore, the inclusion of σ_{KJ} had less effect on the rate of convergence of the fit. The standard deviations for the millimeter wave and FTMW data were 33.0 kHz and 1.2 kHz, respectively, values which are practically identical to those in reduction D. For both fits, only a very few of the more than 200 pairwise correlation coefficients exceed a value of 0.9 (8 in reduction D

TABLE 5: Demonstration of Unitary Equivalence of Parameter Sets Obtained for Reduction *D* and Model II in the Vibrational State $v_5 = 1$ of NSF_3

term[a]	unit	verification
Δq_{12}	MHz	−0.326070 (23)
$[FA\zeta\Delta\varepsilon]/[2q_{22}(A - B)]$	MHz	−0.3264966 (4)
$\Delta\eta_J$	kHz	5.7634 (11)
$-\Delta\eta_K$	kHz	5.696 (153)
$2\Delta B$	kHz	5.692 (463)
$-\Delta A$	kHz	5.710 (815)
$4A\zeta\varepsilon_0(q_{12}^D + q_{12}^{II})/[q_{22}(A - B)]$	kHz	5.772 (39)
Δf_{22}^J	Hz	2.17168 (95)
Δf_{42}	Hz	2.16657 (25)
$[\varepsilon_0/(A - B)][(A\zeta\varepsilon_0/2q_{22}) + q_{12}^D + q_{12}^{II}]$	Hz	2.169 (15)
Δh_3	mHz	0.1635 (28)
$\Delta\varepsilon^2/(A - B)$	mHz	0.1626 (20)

[a] $F = A - B + 2A\zeta$. [b] $\Delta P = P^{II} - P^D$.

and 7 in model II), with none exceeding 0.99. The results of both fits are given in Table 4. The corresponding reproduction of the transition frequencies is given in Table S2 of the Supporting Information.

Again it is useful to check the unitary equivalence of the parameter sets. As already pointed out, the data sets cannot be correctly reproduced with reductions *Q* and *QD*, and we will not consider these reductions further. Thus we are left with checking the unitary equivalence of the parameter sets determined for reduction *D* and model II. The standard deviations determined with these models are nearly identical. Relations for checking the unitary equivalence between these two models can easily be obtained using results given in refs 1 and 2.

$$\Delta q_{12} = \frac{FA\zeta}{2q_{22}(A-B)}\Delta\varepsilon \tag{4}$$

$$\Delta\eta_J = -\Delta\eta_K = 2\Delta B = -\Delta A = 4[q_{12}^D + q_{12}^{II}]\frac{A\zeta\varepsilon_0}{q_{22}(A-B)} \tag{5}$$

$$\Delta f_{22}^J = \Delta f_{42} = \frac{\varepsilon_0}{A-B}\left[\frac{A\zeta\varepsilon_0}{2q_{22}} + q_{12}^D + q_{12}^{II}\right] \tag{6}$$

where $F = (A - B + 2A\zeta)$ and ΔP now corresponds to the difference $(P^{II} - P^D)$ in the parameter values obtained with model II and reduction *D*. The results presented in Table 5 demonstrate that the unitary equivalence relations are fulfilled. In general, good agreement is found for all the relationships. Clearly, for eq 4 which provides the lowest order comparison, the values differ by many times the statistical error σ. However, 3σ is very small in this case: only ∼200 ppm. There will be higher order corrections to the contact transformations used, and the resulting contributions might be significantly larger than this rather small value of 3σ. On the other hand, the relations in eq 5 are fulfilled to within the 1σ limit. Some of the values obtained have larger relative errors, for ΔA up to nearly 50% (3σ), but astonishingly all expressions in eq 5 agree within 2%. In eq 6, the differences experimentally obtained agree with their calculated counterparts, but they exceed the 3σ limit slightly if compared directly. The relation involving the parameter h_3 taken from eq 1 is fulfilled to within 1σ. The relations involving τ-constants have also been tested, but were not fulfilled. This might be explained by the correlation of τ_K with σ_{KJ}.

The results demonstrate the validity of the models applied. Consequently, the parameters obtained can be considered as reliable, except possibly those of highest order. Furthermore, this check confirms the validity of the effective Hamiltonian for an isolated degenerate vibrational state. Thus the failure in fitting the data using reductions *Q* and *QD* cannot be explained by resonant interactions with levels from other vibrational states. A possible explanation must then be found in the transformation properties of the free contact transformation within the ($v_5 = 1$) vibrational state itself.

5. Discussion

Failure of Reductions *Q* and *QD*. Here we would like to discuss how the theory of reduction could explain or provide indications why the reductions *Q* and *QD* fail to reproduce the experimental data. In this discussion, it is necessary to focus our attention on the parameters *t* and *s* that characterize the lowest order contact transformation. In particular, we require the expressions that relate the transformation parameters *t* and *s* to the molecular constants that appear in the untransformed Hamiltonian, constants whose values could lead to a violation of the order-of-magnitude limits on *t* and *s* and thus lead to a slow convergence of the reduced effective Hamiltonian.[1]

Consider the three lower order off-diagonal parameters q_{12}, ε, and d_t. For each of these parameters, the value $\tilde{P}$ after the application of the contact transformation is related to the value *P* that appears in the untransformed Hamiltonian through relationships that involve *t* and *s*, as well as other molecular parameters in the untransformed Hamiltonian. It has been shown that[2]

$$\tilde{q}_{12} = q_{12} + \frac{1}{2}Fs \tag{7a}$$

$$\tilde{\varepsilon} = \varepsilon + 3(A-B)t \tag{7b}$$

$$\tilde{d}_t = d_t + 2q_{22}s - 6A\zeta t \tag{7c}$$

The definitions of the transformation parameters *t* and *s* depend on the reduction chosen which in turn is defined by the constraints applied to q_{12}, ε, and d_t. With constraints indicated below, one defines the reduction (*Q*, *D*, or *QD*) and obtains the associated expressions for the transformation parameters *t* and *s*:

$$q_{12}^Q = q_{12}^{QD} = 0 \rightarrow s^Q = s^{QD} = -2\frac{q_{12}}{F} \tag{8a}$$

$$\varepsilon^Q = \varepsilon^D = 0 \rightarrow t^Q = t^D = -\frac{\varepsilon}{3(A-B)} \tag{8b}$$

$$d_t^D = 0 \rightarrow s^D = -\frac{1}{2q_{22}}\left[d_t + 2\frac{A\zeta}{A-B}\varepsilon\right] \tag{8c}$$

$$d_t^{QD} = 0 \rightarrow t^{QD} = \frac{1}{6A\zeta}\left[d_t - 4\frac{q_{22}q_{12}}{F}\right] \tag{8d}$$

In addition, one finds that[2]

$$d_t^Q = d_t - \frac{4q_{22}q_{12}}{F} + \frac{2A\zeta}{A-B}\varepsilon \tag{9a}$$

$$q_{12}^D = q_{12} - \frac{F}{4q_{22}}\left[d_t + 2\frac{A\zeta}{A-B}\varepsilon\right] \tag{9b}$$

$$\varepsilon^{QD} = \varepsilon + \frac{A-B}{2A\zeta}\left[d_t - 4\frac{q_{22}q_{12}}{F}\right] \tag{9c}$$

From these expressions, one has to estimate the order of magnitude of the transformation parameters *t* and *s,* and consequently one has to know the values of the parameters appearing in the unreduced effective Hamiltonians. Since there is no knowledge about the values of the true parameters q_{12}, d_t, and ε, one has to assume that they are at the order of magnitude

TABLE 6: Molecular Parameters (MHz) Relevant for the Calculation of Free Transformation Parameters for Selected Molecules and Vibrational States[a]

molecule	vibr state	$\|3(A-B)\|$	$\|F/2\|$	$\|2q_{22}\|$	$\|6A\zeta\|$	ref
NSF_3	$v_5 = 1$	*1659*	*883*	*3.3*	*6954*	6
NSF_3	$v_6 = 1$	*1649*	*1089*	*0.5*	*4877*	6
OPF_3	$v_5 = 1$	*600*	*625*	*1.3*	*3150*	14
OPF_3	$v_6 = 1$	*624*	*606*	*0.5*	*4260*	14
CDF_3	$v_5 = 1$	12783	2042	**1.1**	*24972*	5
CH_3CF_3	$v_{12} = 1$	965	1681	3.8	*9124*	20
$SiHF_3$	$v_4 = 1$	9201	912	7.3	14670	21
$FClO_3$	$v_6 = 1$	*1097*	1964	5.3	10684	19

[a] For oblate tops, the parameter A in the table needs to be exchanged by C.

required for the model to be valid. If this assumption is fulfilled, one is left to check the absolute values of $F/2$, $2q_{22}$, $6A\zeta$, and $3(A - B)$. These four constants appear in the denominators in eq 8; if they are too small, the order-of-magnitude requirements will not be met. In order to judge whether the values of these constants for NSF_3 in $v_5 = 1$ are too small or not, we have collected values of these four parameters in Table 6 for various molecules in different degenerate vibrational states $v_t = 1$. One criterion for the selection was that the vibrational states should have been investigated under high resolution and various reductions should have been applied. Table 6 furthermore contains parameters of the related molecules OPF_3 and CH_3CF_3 which are of particular interest because they are closely related to NSF_3. Of the parameters in Table 6, only those which are neither bold nor italic do not—according to the published analyses—lead to a violation of the order-of-magnitude limits for the transformation parameters. Those included in **bold** clearly lead to a violation, and for those included in *italics* no significant information is available (e.g. the corresponding reduction has not been applied). From an inspection of Table 6, for NSF_3 in the state $v_5 = 1$ only the absolute values of $3(A - B)$ and $F/2$ are clearly relatively small and therefore may lead to a violation of the order-of-magnitude requirements. The absolute values of q_{22} and $6A\zeta$ are large enough so that no problems should be expected from the constraint $d_t = 0$ in reductions D and QD, respectively, (see eqs 8c and 8d). The conclusion with regard to reduction D is confirmed by the fact that this is the only reduction for which the data could be fit successfully. This experimental result also leads to the conclusion that the second constraint in reduction D, $\varepsilon = 0$, does not cause problems either. This deduction is supported by the results obtained in the ground vibrational state where the same constraint has been applied in reduction A. It follows then that the small value of $|3(A - B)|$ does not introduce any serious difficulties with the application of reduction Q. Finally, we can conclude that the primary reason for the failure of reductions Q and QD is the relatively small value of $|F/2|$. This is surprising since $|F/2|$ for $SiHF_3$ in the $v_4 = 1$ state takes a similar value and the other constants for this case are in general larger than their counterparts for $v_5 = 1$ in NSF_3. Thus, with respect to the order-of-magnitude considerations, the value of $|F/2|$ for $SIHF_3$ has to be considered to be more critical than the NSF_3 value relevant to the reductions applied here, but nevertheless all reductions could be performed equally well.

It is interesting to discuss the analysis and results obtained for NSF_3 in the $v_6 = 1$ vibrational state by Small and Smith.[6] As mentioned in the Introduction, in their analysis of data which included measurements of both millimeter wave R-branch lines and radiofrequency perturbation-allowed $\Delta k = \pm 3$ transitions, q_{12} and $\tau_{xxxz} = 4\varepsilon$ were fitted simultaneously, a process which is in disagreement with the theory of reduction. To understand their analysis, it is necessary to keep in mind that, when their work was done, the theory of reduction had not been developed yet. Small and Smith believed that the inclusion of ε or d_t is equivalent for their experimental data set, and furthermore they did not question the possibility of fitting one of these together with q_{12}. In fact, as stated in ref 6, the inclusion of both q_{12} and τ_{xxxz} was necessary to obtain a good fit to the data. An explanation for this choice can be seen from the parameters given in Table 6. Clearly the largest difference between the parameters for the $v_6 = 1$ and $v_5 = 1$ states is the much smaller value of $|2q_{22}|$ for the $v_6 = 1$ state. This small value can lead to a violation of the order-of-magnitude limits if the constraint $d_t = 0$ is applied to define the transformation parameter s (see eq 8c). Since Small and Smith did not consider fitting d_t, the parameters to be fitted had to be chosen in such a way that the constraint $d_t = 0$ defines the transformation parameter t rather than s. It follows then that τ_{xxxz} had to be fitted, and this corresponds to reduction QD. Since fitting the data only with τ_{xxxz} was not sufficient, the value of $|F/2|$ must be too small to allow q_{12} to be constrained to zero, a result already obtained for $v_5 = 1$. The transformation parameter s might have been defined by the constraint $\eta_K = 0$, but this is rather awkward. It is worth noting that the fact τ_{xxxz} had to be included in the fit does not follow from the small value of $|3(A - B)|$.

There is another interesting feature which can be taken from Table 6 with regard to OPF_3. For both vibrational states, it seems that none of the well-known reductions can be applied. The relatively small value of $|3(A - B)|$ prevents ε from being constrained to zero, so that both reductions Q and D can be expected to fail to reproduce the data. Furthermore, the small value of $|F/2|$ should lead to problems in reductions Q and QD. It then seems to be necessary for both states to fix ε to the ground-state value and to fit q_{12}. For the $v_5 = 1$ state, d_t can be constrained to zero (the resulting model corresponds to model II used in this work). However, this choice might not be possible for $v_6 = 1$ because of the small value of q_{22}. It might be interesting for the understanding of the application of models of reduction to reinvestigate these two states of OPF_3.

Regional Resonances. In the Introduction, we have introduced the term "regional resonance" for the process in which a cluster of several closely spaced energy levels strongly interacts for a large number of J-values. This process leads to the observation of several series of perturbation-allowed transitions. We have introduced the term to distinguish this particular type of resonance from its global and local counterparts. Global resonances involve levels interacting over a wide range in J, but the number of strongly interacting levels is typically smaller (most commonly only two) and the coupling increases with J, an example being the resonances due to the (2,2) interaction. Local resonances involve typically two accidentally near-degenerate levels which interact strongly only over a very narrow range in J. In general, the resulting shifts of local resonances are clearly visible in Fortrat diagrams and energy level schemes. On the contrary, in the Fortrat diagram for the Q-branch transitions observed in the present work (see Figures 2 and 3), we notice that the reduced energy plots themselves are rather smooth, but there are sudden changes in the labeling, changes which are caused by the "regional resonance".

In the following, we would like to pay particular attention to the situation in NSF_3 of interest here, by considering the development with J of the relative position of the energy levels in regional resonance, and the development of the decomposition of the corresponding eigenvectors in terms of the usual

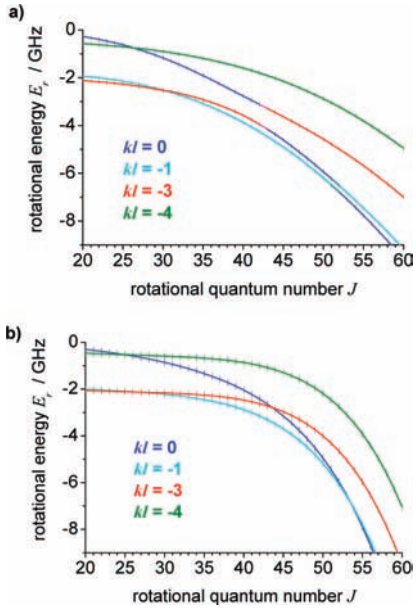

Figure 5. Relative position of the energy levels $kl = 0$, -1, -3 and -4 for NSF_3 ($\upsilon_5 = 1$). Calculated with (a) all off-diagonal interaction terms or (b) with the (2,2) interaction as the only off-diagonal interaction.

symmetric top basis functions. In Figure 5a, we have plotted the reduced energy (pure vibrational and rotational terms neglected) and consequently the relative position of the four lowest lying levels of E-symmetry (within a J-block) against the quantum number J. The levels change their relative positions upon change in J and two crossings are easily detected, both associated with local resonances. The first one is between the two higher levels shown in Figure 5a, namely those with $kl = -4$ and $kl = 0$ at $J = 26/27$. The second one is a crossing of the two lower levels, namely those with $kl = -3$ and $kl = -1$ at $J = 30/31$. The first crossing allowed the observation of the perturbation-allowed transitions with selection rule $(kl = +2) \leftrightarrow (kl = -4)$. The second crossing leads to even larger frequency shifts, and perturbation-allowed transitions could be observed following the selection rule $(kl = +3) \leftrightarrow (kl = -3)$ for $J =$ 30,31.

There are two additional changes in the relative ordering of the two lower levels, both caused by the regional resonance. However, these are not as obvious as the ordering changes associated with the two crossings mentioned above and they are only noticed when following the labeling of the states. The $kl = -3$ and $kl = 0$ levels change their relative position at $J =$ 42/43, and the $kl = -1$ and $kl = 0$ levels at $J = 51/52$. The levels have been labeled by their dominant basis function. These changes appear to be somewhat mysterious since it is difficult to find any indication of the labeling change from the relative positions of the associated levels, and it is impossible to identify J-value for the changes from the plot. Note that for J ≥ 35 the three lowest levels in Figure 5a are shown as levels **a**, **b**, and **c** in order of increasing energy in Figure 4.

In Figure 5a, starting at low values of J, one can easily follow the levels at the crossing of $kl = -4$ and $kl = 0$, and at the crossing of $kl = -3$ and $kl = -1$. At higher values of J, the three lowest levels stay in rather stable relative positions, not indicating any additional energy shift. Nonetheless, the labeling changes. Furthermore, as further fits revealed (not shown here), the labeling depends on the reduction or model chosen. The labeling indicated in Figure 5a was derived using reduction D. To give more insight into this change of labeling, we consider

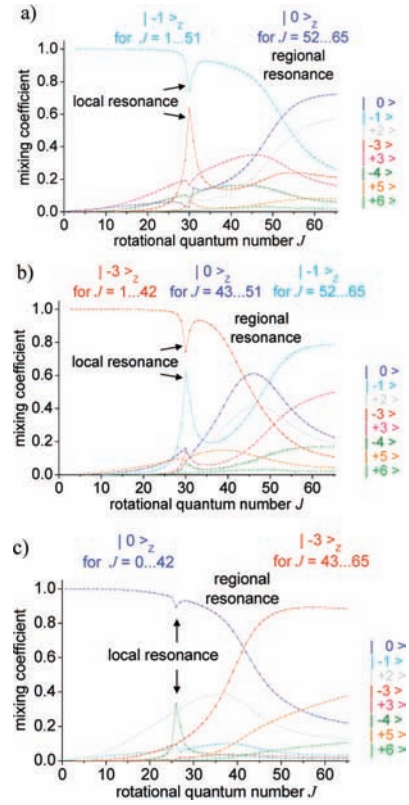

Figure 6. (a−c) Contribution of basis states to the levels a, b, and c ($kl = 0$, -1, -3) of NSF_3 ($\upsilon_5 = 1$).

the mixing coefficient $c_{ij} = \langle i|j\rangle_Z$ which represents the contribution of the basis state $|i\rangle$ to the eigenstate $|j\rangle_Z$. Figure 6 shows $|c_{ij}|$ as a function of J for three selected levels ($kl = 0$, -1, -3). Except for the above-mentioned crossings at $J = 26/27$ and $J = 30/31$, we follow the levels in Figure 6 according to their relative position in Figure 5a, and not according to their labeling by their dominant basis function. The method adopted for following the levels in Figure 6 corresponds to the levels connected by solid lines in Figure 5a. For example, the contribution of basis states is shown in Figure 6a for the lowest level for $J < 31$ and the second lowest for $J \geq 31$.

Inspecting Figure 6, one can easily recognize the local resonance at $J = 30/31$ from the peaks in the contributions of the $|kl = -3>$ and $|kl = -1>$ basis states in Figures 6a and 6b, respectively. Similarly, the resonance at $J = 26/27$ can be easily recognized from the peak of the contribution of the $|kl = -4\rangle$ basis state in Figure 6c. For higher values of J, the levels are strongly mixed; especially for J between 35 and 65, several basis states contribute to the eigenstates of the corresponding levels. In this range in J, we use the term regional resonance where typically more than two basis states are contributing to the eigenstates over a large range of J-values. At even higher values of J, the resonance becomes global in nature. The (2,2) interaction provides the strongest mixing, and consequently each eigenstate consists primarily of two basis states with $|\pm k, l = \mp 1\rangle$ and $|\pm(k + 2), l = \pm 1\rangle$. In particular in Figure 6a, the basis states $|kl = 0\rangle$ and $|kl = +2\rangle$ are dominant; in Figure 6b $|kl = -1\rangle$,$|kl = +3\rangle$; and in Figure 6c, $|kl = -3\rangle$,$|kl = +5\rangle$.

The different resonances lead to different types of transitions. The local resonances for $J = 26/27$ and $J = 30/31$ are due to the $(2, -4)$ interaction which made possible the observation of perturbation-allowed transitions with selection rule $\Delta(k - l) = \pm 6$. These particular resonances occur because the first order energy differences ΔE between the levels connected by the (2,

-4) interaction are accidentally very small ($\Delta E = 4(k + 1)[(2(A - B) + A\zeta)]$ with $(2(A - B) + A\zeta) = -52$ MHz and k corresponding to the level with $kl < 0$). The global resonance induced by the (2,2) interaction allows the observation of direct l-type resonance transitions with $\Delta(k - l) = 0$ for $J > 15$ and $G = 0$ to 3. The limitation in J and G is mainly due to the spectral ranges covered by the spectrometers used and the weaker (2,2) interaction at low J. For the regional resonances, an interplay of practically all the off-diagonal interactions leads to strong mixing with several basis states contributing. Because of this, it was possible to observe a large number of $\Delta(k - l) = \pm 3$ and ± 6 perturbation-allowed transitions following various detailed selection rules. For E-symmetry, six types of transitions (four in addition to the two direct l-type resonance transitions) should be observable due to the strong mixing and are predicted for the spectral range covered. Five of these have been measured for several values of J. For example, the observation of the transitions with $(kl = +3) \leftrightarrow (kl = 0)$ was only limited by the spectral range (18−26.5 GHz) of the spectrometer employed. Measurements of transitions following the selection rule $(kl = +3) \leftrightarrow (kl = -3)$ were only successful for $J = 41$ and 42. For these values of J, the $kl = -3$ level is at lower energy than the $kl = 0$ level and the $(kl = +3) \leftrightarrow (kl = -3)$ transitions are the extension to lower frequencies of the $(kl = +3) \leftrightarrow (kl = 0)$ series, see Figure 3b (in this discussion, the transitions observed for $J = 30$ and 31 are not considered because these are due to a local resonance).

For both A_1 and A_2 symmetries, the situation is quite similar, but the number of perturbation-allowed transitions observed for each series was even larger because significantly more transitions fall into the spectral range covered.

Calculations with the (2,2) interaction as the only off-diagonal interaction included are shown in Figure 5b. It is seen, for example, that a crossing of the $kl = -1$ and $kl = 0$ levels is predicted at $J = 53/54$, whereas in reality this crossing does not occur. The comparison with Figure 5a leads to the conclusion that the other off-diagonal interactions just balance the effect of the (2,2) interaction in the region of the regional resonance. As a result, the energy levels stay more or the less in the same relative position, with their spacing being rather stable. This competition of interactions leads to the strong mixing of several basis states. The effect is very pronounced for the lowest lying levels of E-symmetry because in this case three interacting levels are relatively close.

Measurements of the hyperfine structure of the "regional resonance" transitions show that the properties of the eigenstates are more sensitive to the relative position of levels than to the identity of the particular one of the many basis states that is dominant. Through the associated range in J, many of the basis states in each of these eigenstates are of comparable importance. The properties of the eigenstates are an average over those of the contributing basis states, and this average changed relatively little when the mixing coefficients change by the small amounts needed to promote a different basis state to the first rank. Consequently, it is more constructive to label the eigenstates by their relative energy (as was done here) rather than their dominant basis function. The conclusion regarding the sensitivity to the relative position is supported by the fact that transitions following the selection rule $(kl = +3) \leftrightarrow (kl = -3)$ could only be measured if the $kl = -3$ level is at lower energy than the $kl = 0$ level. Transitions from the $kl = +3$ level to the upper level with $kl = -3$, $kl = -1$, and $kl = 0$ could not be observed.

Parameters Determined in the Two Chosen Models. All parameters determined in both the ground and $\upsilon_5 = 1$ vibrational states are of the correct order of magnitude except the L constants. The internal consistency of most of the parameters has carefully been tested and verified using relations resulting from the theory of reduction.

The regional resonance in the $\upsilon_5 = 1$ vibrational state allowed the precise determination of the A rotational constant. The precision obtained is similar to that in previous investigations (see, e.g., ref 1). However, because the measured transitions sampled a considerable variety of different selection rules, the value of A shows a correlation with $A\zeta$ that is smaller than usual: 0.92 as compared to typical values of 0.99. The presently determined value of A as given in Table 4 is significantly larger and more precise than those obtained by Small and Smith[6] for $\upsilon_5 = 1$ (5182 MHz) and for $\upsilon_6 = 1$ (5178 MHz).

The constants D_J and D_{JK} are well determined (error ≤ 100 ppm) in the ground and the $\upsilon_5 = 1$ states, and are in good agreement with those reported in ref 6. The regional resonance allowed the determination of D_K, which is in general not possible for direct l-type resonance spectra even if strong local resonances affect the observed transitions. This parameter is well determined (error ∼1%) and shows no strong correlation with any other parameters. The constants H_J, H_{JK}, and H_{KJ} were determined in the ground-state with a precision of about 2−4%. The results for the L constants in the $\upsilon_5 = 1$ state should be considered as effective values. The parameters of off-diagonal centrifugal distortion terms, ε and h_3, are well determined. The values of h_3 obtained in the ground-state and the $\upsilon_5 = 1$ excited state (reduction D) differ by roughly 20%.

The lower order z-Coriolis constants $A\zeta$, η_J, and η_K are well determined and show no severe correlations (correlation coefficients ≤0.97). Compared to the result of −1169.4 MHz in ref 6, the present value of −1158.8 MHz for $A\zeta$ differs considerably which parallels the result for A. For the higher order z-Coriolis constants (τ, σ), the set obtained in model II seems to be more reliable since the correlation between τ_K and σ_{KJ} is less pronounced. The precision is between 0.3% and 3%.

Finally, the parameters of the off-diagonal (2,2), (2,−1) and (2,−4) interactions have been precisely determined. The accuracy is better than 0.001% at second order (q_{22}, q_{12}); better than 0.1% at fourth order (f_{22}^J, f_{22}^K, f_{42}, f_{12}^J); and better than 1% at sixth order (f_{22}^{JJ}, f_{42}^J). Thus even at sixth order, the constants have been accurately determined.

A comment should be made about the relative signs of the off-diagonal parameters of the molecular Hamiltonian of the degenerate $\upsilon_5 = 1$ level. It is well established[22] that, from the direct analysis of only rotational data, it is not possible to determine the absolute sign of the leading parameter q_{22} of the (2,2) l-type interaction and consequently its expansion terms. In addition, according to the phase conventions discussed in ref.,[22] the sign of the parameter f_{42} is linked to the sign of q_{22}. These sign relations can be represented by the arbitrary factor $\varepsilon_2 = \pm 1$ used in Tables 3 and 4 of ref.[22] In a similar manner, only the relative signs of the parameters q_{12}, ε, and d_t for the interactions with $\Delta(k - l) = \pm 3$ can be determined. The sign ambiguity of q_{22} can be resolved by analyzing infrared data when the ${}^rQ_0$ branch and one of the ${}^rP_0/{}^rR_0$ branches can be assigned. Unfortunately, the ${}^rQ_0$ branch is frequently congested and of no use in this regard. In such a situation, one can often still determine the sign of q_{22} by simulating the intensity distribution in the perpendicular vibration−rotation band.

In the present case, only rotational data are available, but reduction theory can provide another method of determining the sign of q_{22}. This method is based on eq 4 that links the difference Δq_{12} in values of the q_{12} parameter in the two

reductions to the difference $\Delta\varepsilon$ in ε for the same two reductions. From this relationship, the sign for q_{22} results as negative from the relative sign of Δq_{12} and $\Delta\varepsilon$ and the known signs of the other parameters in eq 4. The important point is that $\Delta\varepsilon$ is fixed and Δq_{12} results from the fits with the relative sign of the differences clearly determined. In the present case the magnitude of ε has been taken from the fit of the ground-state data. Furthermore, it has been assumed that the sign of ε is known, as positive in this case, as follows from the sign assumed for the ground state (see section 4). However, the theory of reduction itself is consistent with the existence of a second parameter set with $\varepsilon > 0$, but in this case q_{12} with opposite sign but with a different magnitude of q_{12}. It is also consistent with parameter sets with $\varepsilon < 0$ which have been discarded beforehand. Any combination of these parameter sets fulfils eq 4 based on a negative sign of q_{22}.

This method to determine the sign of q_{22} can be applied to any symmetric top molecule with C_{3v} symmetry in the degenerate vibrational state $v_t = 1$. Besides the fits following the standard reductions a fit has to be performed with one parameter of a $\Delta(k - l) = 3$ interaction fixed. In case the fixed parameter is ε, eq 4 can be used to determine the sign of q_{22}, in case q_{12} or d_t are the parameters fixed, the corresponding relations might be obtained from eq 7.

6. Conclusion

We have investigated the rotational spectra of NSF_3 in the ground and $v_5 = 1$ vibrational states to test the applicability of models of reduction of the effective Hamiltonian to a molecule which is close to a spherical top, but not an extreme case. For the ground state, the R-branch data set was extended significantly, but no Q-branch transitions could be observed. The standard models with the $\Delta k = \pm 3$ interaction (reduction A) or $\Delta k = \pm 6$ interaction (reduction B) constrained to zero were applied successfully. Both models led to practically the same quality of fit and the unitary equivalence of both parameter sets has been demonstrated. In contrast to the related molecule OPF_3 which is closer to the spherical-top limit, the value of $A - B$ is not small enough to lead to a violation of the order-of-magnitude limits for the transformation parameter t, a violation which would not have allowed the application of the constraint $\varepsilon = 0$.

The $v_5 = 1$ vibrational state shows anomalies in the rovibrational structure. The clustering of levels at low K leads to a regional resonance extending over a large range of J, which in turn allows the observation of a considerable number of Q-branch perturbation-allowed transitions. In addition, R-branch transitions and direct l-type resonance transitions have been observed. The analysis of the data shows that models using q_{12} constrained to zero (reductions Q and QD) fail to reproduce the transition frequencies measured. This can be explained as being due to the small absolute value of $F = (A - B + 2A\zeta)$ which makes the transformation parameter s exceed its order-of-magnitude limits. Using reduction D, the data set was reproduced very well showing that the constraints $\varepsilon = 0$, $d_t = 0$ can be applied. This is in agreement with the result obtained for the ground-state with respect to the constraint $\varepsilon = 0$. Furthermore, an alternative model with $d_t = 0$ and ε constrained to the ground-state value obtained with reduction B was applied to test the internal consistency. This second model proved to work equally well and it has been demonstrated that the parameter sets of both models are unitary equivalent.

Acknowledgment. We thank Prof. I. Ozier for fruitful discussion and critically reading the manuscript which led to considerable improvements, and Prof. R. Mews for kindly providing the NSF_3 sample. The members of the Kiel group thank the Deutsche Forschungsgemeinschaft and the Fonds der Chemie for funds. P.P. wishes to thank the Grant Agency of the Czech Republic (project AA400400504), the Academy of Sciences of the Czech Republic (project 1ET400400410), the Ministry of Education, Youth and Sports of the Czech Republic (research program LC06071), and the Grant Agency of the Academy of Sciences of the Czech Republic (project IAA400400706) for support.

Appendix

The Hamiltonian employed in the calculations of vibration−rotation levels had the following form. The diagonal matrix elements up to sixth order were taken as follows:

$$E^0_{vr}(J,k,l) = E_v + B_v J(J+1) + (A_v - B_v)k^2 - D^v_J J^2(J+1)^2 - D^v_{JK} J(J+1)k^2 - D^v_K k^4 + H^v_J J^3(J+1)^3 + H^v_{JK} J^2(J+1)^2 k^2 + H^v_{KJ} J(J+1)k^4 + H^v_K k^6 + L^v_J J^4(J+1)^4 + L^v_{JJK} J^3(J+1)^3 k^2 + L^v_{JK} J^2(J+1)^2 k^4 + L^v_{JKK} J(J+1)k^6 + L^v_K k^8 + [-2(A\zeta)_v + \eta^v_J J(J+1) + \eta^v_K k^2 + \tau^v_J J^2(J+1)^2 + \tau^v_{JK} J(J+1)k^2 + \tau^v_K k^4 + \sigma^v_J J^3(J+1)^3 + \sigma^v_{JK} J^2(J+1)^2 k^2 + \sigma^v_{KJ} J(J+1)k^4 + \sigma^v_K k^6]kl \quad \text{(A1)}$$

Clearly, the l-dependent terms apply only to the $v_5 = 1$ vibrational state. For ($v_5 = 1$), the following off-diagonal matrix elements of l-type operators were taken into account:

$$\langle v_t^{l\pm2}; J, k \pm 2|H_{22} + H_{24} + H_{26}|v_t^l; J, k\rangle = 2\{q_{22} + f^J_{22} J(J+1) + f^K_{22}[k^2 + (k \pm 2)^2] + f^{JJ}_{22} J^2(J+1)^2\} F^{\pm}_2(J,k) \quad \text{(A2)}$$

$$\langle v_t^{l\mp2}; J, k \pm 1|H_{22} + H_{24}|v_t^l; J, k\rangle = 2[q_{12} + q^J_{12} J(J+1)] \times (2k \pm 1) F^{\pm}_1(J,k) \quad \text{(A3)}$$

$$\langle v_t^{l\mp2}; J, k \pm 4|H_{24} + H_{26}|v_t^l; J, k\rangle = 2[f_{42} + f^J_{42} J(J+1)] F^{\pm}_4(J,k) \quad \text{(A4)}$$

For both states studied, matrix elements of the operator for the ($\Delta k = \pm 3$) interaction was taken in the form

$$\langle v_t^l; J, k \pm 3|H_{04}|v_t^l; J, k\rangle = \varepsilon(2k \pm 3) F^{\pm}_3(J,k) \quad \text{(A5)}$$

and of the operator for the ($\Delta k = \pm 6$) interaction in the form

$$\langle v_t^l; J, k \pm 6|H_{06}|v_t^l; J, k\rangle = h_3 F^{\pm}_6(J,k) \quad \text{(A5a)}$$

The matrix elements of rotational shift operators were taken in the conventional form as follows:

$$F^{\pm}_n(J,k) = \prod_{i=1}^{n} [J(J+1) - (k \pm i \mp 1)(k \pm i)]^{1/2} \quad \text{(A6)}$$

Supporting Information Available: Text file giving the spectral data (frequencies of transitions) for the ground and the $v_5 = 1$ vibrational state, denoted as S1 and S2, respectively. This material is available free of charge via the Internet at http://pubs.acs.org.

References and Notes

(1) Sarka, K.; Papoušek, D.; Demaison, J.; Mäder, H.; Harder, H. In *Vibration-Rotational Spectroscopy and Molecular Dynamics*; Papoušek,

D., Ed.; Advanced Series in Physical Chemistry 9; World Scientific: Singapore, 1997; p 116.

(2) Harder, H. *J. Mol. Spectrosc.* **1999**, *194*, 145.

(3) Styger, C.; Ozier, I.; Bauder, A. *J. Mol. Spectrosc.* **1992**, *153*, 101.

(4) Fusina, L.; Di Lonardo, G.; De Natale, P. *J. Chem. Phys.* **1998**, *109*, 997.

(5) Pracna, P.; Sarka, K.; Demaison, J.; Cosléou, J.; Herlemont, F.; Khelkhal, M.; Fichoux, H.; Papoušek, D.; Paplewski, M.; Bürger, H. *J. Mol. Spectrosc.* **1997**, *184*, 93.

(6) Small, C. E.; Smith, J. G. *Mol. Phys.* **1979**, *37*, 665.

(7) Small, C. E.; Smith, J. G.; Whiffen, D. H. *Mol. Phys.* **1979**, *37*, 681.

(8) Butcher, R. J.; Chardonnet, Ch.; Borde, Ch. J. *Phys. Rev. Lett.* **1993**, *70*, 2698.

(9) Manuscript in preparation; see also: Macholl, S., Harder, H., Mäder, H., Fusina, L., Ozier, I. *19th International Conference on High Resolution Molecular Spectroscopy*; Prague, Czech Republic, August 29 - September 2, 2006, post deadline paper H61.

(10) Krüger, M.; Harder, H.; Gerke, C.; Dreizler, H. *Z. Naturforsch.* **1993**, *48a*, 737.

(11) Meyer, V.; Jäger, W.; Schwarz, R.; Dreizler, H. *Z. Naturforsch.* **1991**, *46a*, 445.

(12) Aliev, M. R.; Aleksanyan, V. T. *Opt. Spectrosk.* **1968**, *24*, 388.

(13) Sarka, K. *J. Mol. Spectrosc.* **1989**, *133*, 461–466.

(14) Smith, J. G. *Mol. Phys.* **1976**, *32*, 621.

(15) Ozier, I.; Schroderus, J.; Wang, S.-X.; McRae, G. A.; Gerry, M. C. L.; Vogelsanger, B.; Bauder, A. *J. Mol. Spectrosc.* **1998**, *190*, 324.

(16) Lobodenko, E. I.; Sulakshina, O. N.; Perevalov, V. I.; Tyuterev, V. G. *J. Mol. Spectrosc.* **1987**, *126*, 159.

(17) Watson, J. K. G.; Gerke, C.; Harder, H.; Sarka, K. *J. Mol. Spectrosc.* **1998**, *187*, 131.

(18) Margulès, L.; Cosléou, J.; Bocquet, R.; Demaison, J.; Mkadmi, E. B.; Bürger, H.; Wötzel, U.; Harder, H.; Mäder, H. *J. Mol. Spectrosc.* **1999**, *196*, 175.

(19) Graner, G.; Meguellati, F.; Ceausu, A.; Burczyk, K.; Pawelke, G.; Pracna, P. *J. Mol. Spectrosc.* **1999**, *197*, 76.

(20) Gerke C. Doctoral Thesis, Kiel, Germany, 1996.

(21) Gnida, M.; Margulès, L.; Cosléou, J.; Bocquet, R.; Demaison, J.; Mkadmi, E. B.; Bürger, H.; Harder, H.; Mäder, H. *J. Mol. Spectrosc.* **2000**, *200*, 40.

(22) Bürger, H.; Cosléou, J.; Demaison, J.; Gerke, C.; Wötzel, U.; Harder, H.; Mäder, H.; Paplewski, M.; Papoušek, D.; Watson, J. K. G. *J. Mol. Spectrosc.* **1997**, *182*, 34.

JP807342F